Reference List

[1] Public Utilities Commission of Sri Lanka, "Net Metering Development in Sri Lanka," 2015.

[2] CEB, "CEB Statistical Digest," 2016. .

[3] S. V. S. Kumary, V. A. Aman, M. Than, G. M. Shafiullah, and A. Stojcevski, "Modelling and Power quality analysis of a Grid-connected Solar PV System," no. October, pp. 5–10, 2014.

[4] Mathworks, "Single-Phase, 240 Vrms, 3500 W Transformerless Grid-Connected PV Array," *Matlab R2017b Documentation*. [Online]. Available: https://www.mathworks.com/help/physmod/sps/examples/single-phase-240-vrms-3500-w-transformerless-grid-connected-pv-array.html.

[5] L. Ma *et al.*, "Leakage Current Analysis of Single-phase Transformer-less Grid -connected PV Inverters," in *IECON*, 2015, pp. 887–892.

[6] T. Kheng, S. Freddy, N. A. Rahim, W. Hew, and H. S. Che, "Comparison and Analysis of Single-Phase Transformerless Grid-connected PV Inverters," vol. 29, no. 10, p. 8993, 2014.

[7] V. Salas, E. Olías, M. Alonso, F. Chenlo, and A. Barrado, "DC current injection into the network from PV grid inverters," *Conf. Rec. 2006 IEEE 4th World Conf. Photovolt. Energy Conversion, WCPEC-4*, vol. 2, no. June, pp. 2371–2374, 2007.

[8] B. Liu, Y. Zha, T. Zhang, and S. Chen, "Solid state transformer application to grid connected photovoltaic inverters," *2016 Int. Conf. Smart Grid Clean Energy Technol. ICSGCE 2016*, pp. 248–251, 2017.

[9] N. C. Foureaux, L. Adolpho, S. M. Silva, J. A. D. S. Brito, and B. D. J. Cardoso Filho, "Application of solid state transformers in utility scale solar power plants," *2014 IEEE 40th Photovolt. Spec. Conf. PVSC 2014*, vol. 2, pp. 3695–3700, 2014.

[10] S. Falcones, X. Mao, and R. Ayyanar, "Topology comparison for solid state

transformer implementation," *IEEE PES Gen. Meet. PES 2010*, pp. 1–8, 2010.

[11] A. Q. Huang and R. Burgos, "Review of Solid-State Transformer Technologies and Their Application in Power Distribution Systems," *IEEE J. Emerg. Sel. Top. Power Electron.*, vol. 1, no. 3, pp. 186–198, 2013.

[12] R. W. a a De Doncker, D. M. Divan, and M. H. Kheraluwala, "A three-phase soft-switched high-power-density DC/DC converter for high-power applications," *IEEE Trans. Ind. Appl.*, vol. 27, no. 1 pt 1, pp. 63–73, 1991.

[13] D. Segaran, D. G. Holmes, and B. P. McGrath, "Enhanced load step response for a bidirectional DCDC converter," *IEEE Trans. Power Electron.*, vol. 28, no. 1, pp. 371–379, 2013.

[14] S. Poshtkouhi *et al.*, "A dual-active-bridge based bi-directional micro-inverter with integrated short-term Li-Ion ultra-capacitor storage and active power smoothing for modular PV systems," *2014 IEEE Appl. Power Electron. Conf. Expo. - APEC 2014*, pp. 643–649, 2014.

[15] H. Tao, A. Kotsopoulos, J. L. Duarte, and M. A. M. Hendrix, "A soft-switched three-port bidirectional converter for fuel cell and supercapacitor applications," *PESC Rec. - IEEE Annu. Power Electron. Spec. Conf.*, vol. 2005, no. 1, pp. 2487–2493, 2005.

[16] S. Falcones, R. Ayyanar, and X. Mao, "A DC-DC Multiport-converter-based solid-state transformer integrating distributed generation and storage," *IEEE Trans. Power Electron.*, vol. 28, no. 5, pp. 2192–2203, 2013.

[17] N. A. Rahim, K. Chaniago, and J. Selvaraj, "Single-phase seven-level grid-connected inverter for photovoltaic system," *IEEE Trans. Ind. Electron.*, vol. 58, no. 6, pp. 2435–2443, 2011.

[18] F. A. Ramírez and M. A. Arjona, "A Space Vector Modulation Algorithm for a Grid-Connected Single-Phase Seven Level Inverter," pp. 2–7.

[19] H. Dehbonei, C. V. Nayar, and L. Borle, "A novel modulation technique for a single phase H-bridge inverter," *Int. J. Electron.*, vol. 91, no. 1, pp. 41–55,

2004.

[20] Mitsubishi Electric, "PV-UD185MF5 185Wp Datasheet." [Online]. Available: https://www.mitsubishielectricsolar.com/images/uploads/documents/specs/UD5_spec_sheet_185W.pdf.

[21] S. M. Ferdous, M. A. Mohammad, F. Nasrullah, A. M. Saleque, and A. Z. M. S. Muttalib, "Design and simulation of an open voltage algorithm based maximum power point tracker for battery charging PV system," *2012 7th Int. Conf. Electr. Comput. Eng.*, no. 2, pp. 908–911, 2012.

[22] B. O. Kang and J. H. Park, "Kalman filter MPPT method for a solar inverter," *2011 IEEE Power Energy Conf. Illinois, PECI 2011*, 2011.

[23] T. Esram and P. L. Chapman, "Comparison of Photovoltaic Array Maximum Power Point Tracking Techniques," *IEEE Trans. Energy Convers.*, vol. 22, no. 2, pp. 439–449, 2007.

[24] Research and Development branch of CEB, "Study on Harmonics Generation by Grid Connected PV Inverters," 2015.

[25] IEEE Power and Energy Society, "IEEE Recommended Practice and Requirements for Harmonic Control in Electric Power Systems," 2014.

[26] Transmission Division of Ceylon Electricity Board, "Grid Code," 2015.

[27] IEEE Standards Coordinating Committee 21, "IEEE Guide for Conducting Distribution Impact Studies for Distributed Resource Interconnection," 2013.

[28] Resource Management Associates (RMA) Pvt Ltd and GEO-NET Umweltconsulting GmbH of Germany, "Technical Assistance Consultant's Report on Sri Lanka Clean Energy and Network Efficiency Improvement Project(Wind and Solar Resource Assessment)," 2013.

[29] A. Algaddafi, K. Elnaddab, A. Al, and A. N. Esgiar, "Comparing the Performance of Bipolar and Unipolar Switching Frequency to Drive DC-AC Inverter," 2016.

[30] U. A. Miranda, M. Aredes, and L. G. B. Rolim, “A DQ synchronous reference frame control for single-phase converters,” *PESC Rec. - IEEE Annu. Power Electron. Spec. Conf.*, vol. 2005, pp. 1377–1381, 2005.

[31] J. F. Sultani, J. A. Gow, and E. Tez, “Modelling, Design and Implementation of D-Q Control in Single-Phase Grid-Connected Inverters for Photovoltaic Systems Used in Domestic Dwellings,” DE MONTFORT UNIVERSITY 2013, 2013.

[32] G. Franceschini, E. Lorenzani, C. Tassoni, and A. Bellini, “Synchronous reference frame grid current control for single-phase photovoltaic converters,” *Conf. Rec. - IAS Annu. Meet. (IEEE Ind. Appl. Soc.*, pp. 1–7, 2008.

[33] B. Crowhurst, E. F. El-Saadany, L. El Chaar, and L. A. Lamont, “Single-phase grid-tie inverter control using DQ transform for active and reactive load power compensation,” *PECon2010 - 2010 IEEE Int. Conf. Power Energy*, pp. 489–494, 2010.

[34] C. Transmission Planning Branch, “Transmission System Expansion Plan 2017-2020,” 2017.

[35] Teshmont Consultants LP, “Transformer Modelling Guide,” 2014.

[36] K. H. Ahmed, S. J. Finney, and B. W. Williams, “Passive filter design for three-phase inverter interfacing in distributed generation,” *5th Int. Conf. Compat. Power Electron. CPE 2007*, vol. XIII, no. 2, pp. 49–58, 2007.

[37] A. Reznik, M. G. Simoes, A. Al-Durra, and S. M. Muyeen, “LCL filter design and performance analysis for small wind turbine systems,” *2012 IEEE Power Electron. Mach. Wind Appl.*, pp. 1–7, 2012.

[38] Manish Bhardwaj and B. Subharmanya., “PV Inverter Design Using Solar Explorer Kit,” 2013.

[39] K. George, “Design and Control of a Bidirectional Dual Active Bridge DC-DC Converter to Interface Solar , Battery Storage , and Grid-Tied Inverters,” 2015.

[40] M. H. Kheraluwala, D. W. Novotny, and D. M. Divan, “Design considerations for high power high frequency transformers,” *21st Annual IEEE Conference on Power Electronics Specialists*. pp. 734–742, 1990.

[41] G. Waltrich, J. L. Duarte, M. A. M. Hendrix, and J. J. H. Paulides, “Three-port bi-directional converter for electric vehicles : focus on high-frequency coaxial transformer Three-Port Bi-directional Converter for Electric Vehicles : Focus on High-Frequency Coaxial Transformer,” no. March, pp. 25–28, 2010.

[42] S. Inoue and H. Akagi, “A bidirectional isolated dc-dc converter as a core circuit of the next-generation medium-voltage power conversion system,” *IEEE Trans. Power Electron.*, vol. 22, no. 2, pp. 535–542, 2007.

[43] P. Systems, “Design of a Three-port Solid State Transformer for High Power applications Guirguis Zaki Guirguis Abdelmessih,” 2015.

[44] D. S. Segaran, “Dynamic Modelling and Control of Dual Active Bridge Converters for Smart Grid Applications,” 2013.

[45] D. Segaran, B. P. McGrath, and D. G. Holmes, “Adaptive dynamic control of a bi-directional DC-DC converter,” *2010 IEEE Energy Convers. Congr. Expo.*, pp. 1442–1449, 2010.

[46] C. Zhao, S. D. Round, and J. W. Kolar, “An isolated three-port bidirectional dc-dc converter with decoupled power flow management,” *IEEE Trans. Power Electron.*, vol. 23, no. 5, pp. 2443–2453, 2008.

[47] S. Uddin, H. Shareef, A. Mohamed, and M. A. Hannan, “An analysis of harmonics from LED lamps,” *2012 IEEE Int. Power Eng. Optim. Conf. PEOCO 2012 - Conf. Proc.*, pp. 182–186, 2012.

Appendix A: PV array datasheet

YL 280 P-35b / 1970x990 SERIES

ELECTRICAL PARAMETERS

Electrical parameters at STC (1,000 W/m², 25°C, AM 1.5 according to EN 60904-3)

Module type		YL 260 P-35b	YL 265 P-35b	YL 270 P-35b	YL 275 P-35b	YL 280 P-35b
Power output	[W]	260.0	265.0	270.0	275.0	280.0
Power output tolerances	[%]	+/- 3	+/- 3	+/- 3	+/- 3	+/- 3
Module Efficiency	[%]	13.3	13.6	13.8	14.1	14.4
Voltage at Pmax, V_{mpp}	[V]	35.0	35.3	35.3	35.5	35.5
Current at Pmax, I_{mpp}	[A]	7.43	7.50	7.65	7.75	7.89
Open circuit voltage V_{oc}	[V]	44.6	44.6	44.8	45.0	45.0
Short circuit current I_{sc}	[A]	8.04	8.15	8.20	8.30	8.35
Max. system Voltage	[V]			1,000 VDC		

Parameters of the thermal characteristics

NOCT (Nominal Operating Cell Temperature)	[°C]	46 +/- 2
Temperature coefficient beta of I_{sc}	[1/K]	+ 0.0006
Temperature coefficient alpha of V_{oc}	[1/K]	- 0.0037
Temperature coefficient gamma of P_{mpp}	[1/K]	- 0.0045

IV CURVES

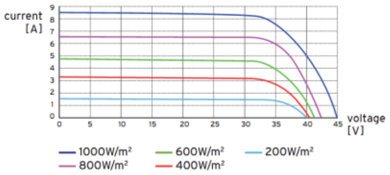

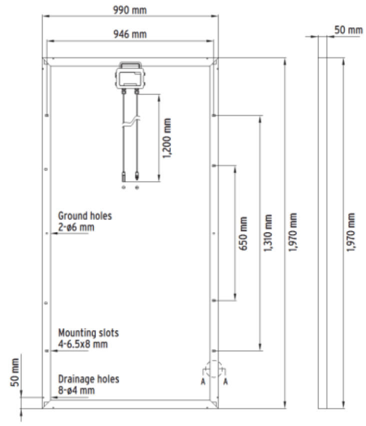

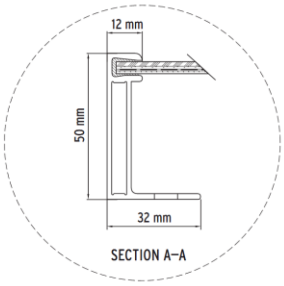

MECHANICAL PARAMETERS

Dimensions (length [mm] / width [mm] / thickness [mm])	1,970 / 990 / 50
Thickness with junction box [mm]	50
Weight [kg]	26.0
Junction box (manufacturer / protection degree / number of diodes)	CIXI / IP65 / 6
Junction box dimensions (length / width / thickness [mm])	151 / 122 / 25
Positive cable & negative cable (manufacturer / length [mm] / cable cross-section [mm²])	CIXI / 1,200 / 4.0
Plug connector (manufacturer / type / protection degree)	MC4 / UV resistance and self-locking / IP67
Front cover (material / thickness [mm])	Tempered Glass, 4.0mm
Cell type (quantity / technology)	72 / polycrystalline / 156 x 156
Encapsulation materials	Ethylene Vinyl Acetate (EVA)
Rear cover (material / thickness [mm])	Le - PET - PVDF / 0.287
Frame (material)	robust anodized aluminum alloy

OPERATING CONDITIONS

Operating temperature [°C]	- 40 to + 85
Max. wind load / Max. snow load [Pa]	2.4K / 5.4K

PACKAGING

Number of modules per box	21
Box size (length [mm] / width [mm] / depth [mm])	1,995 / 1,130 / 1,131
Box Gross weight in kg	586
Boxes per pallet	1

Electrical equipment, check with your installer

* The data does not refer to a single module and they are not part of the offer, they serve for comparison only to different module types.

Yingli Green Energy Holding Co. Ltd.
commerce@yinglisolar.com
0086 - (0)312 - 8929802

Subject to modifications and errors

DS-YL280P-35b-EU-EN-200908-A153-v01

YINGLI SOLAR Power Your Life

www.yinglisolar.com

Appendix B: Simulink model -Transformerless inverter

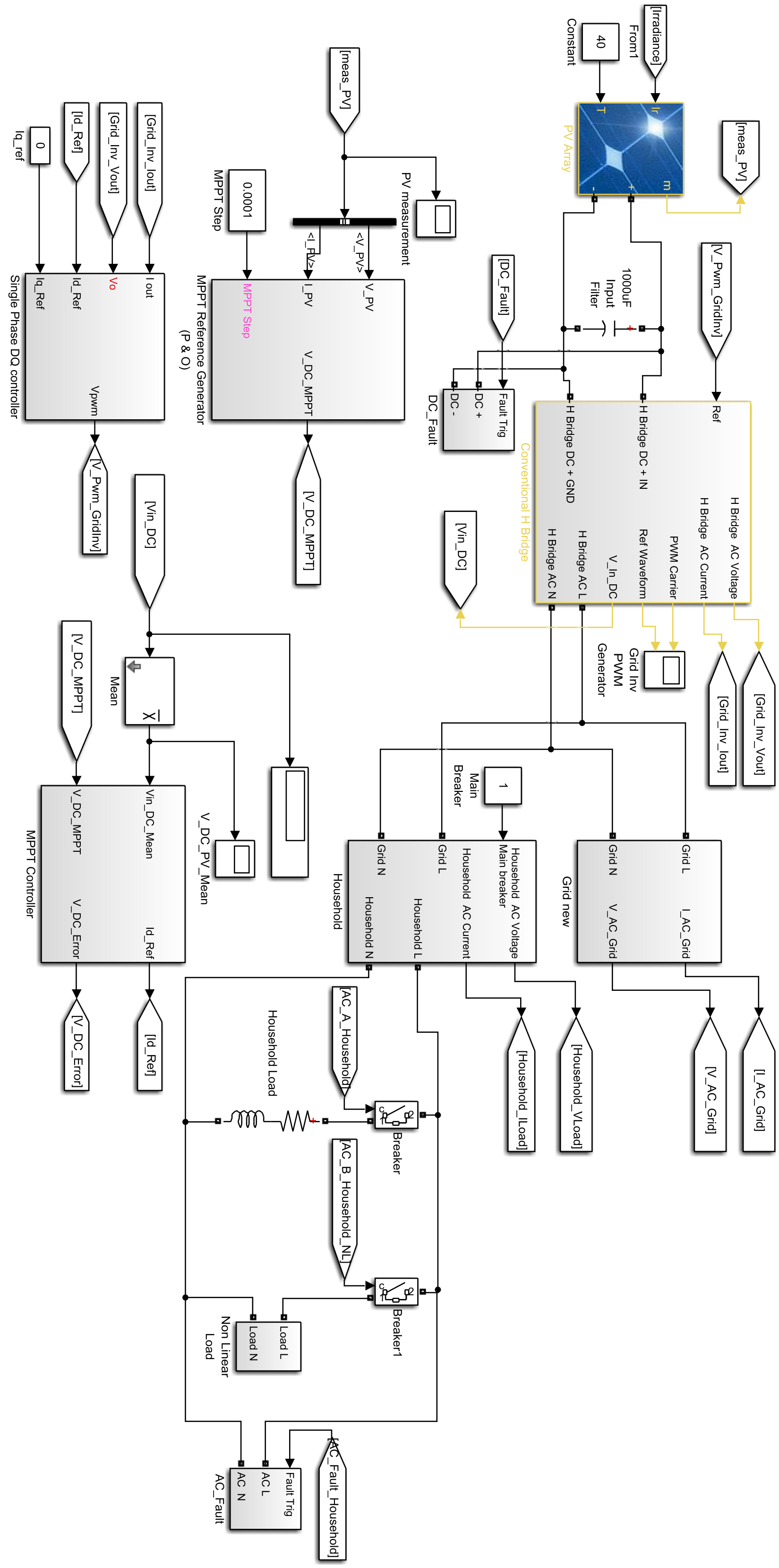

Appendix C: Simulink model-DAB inverter (load at grid side)

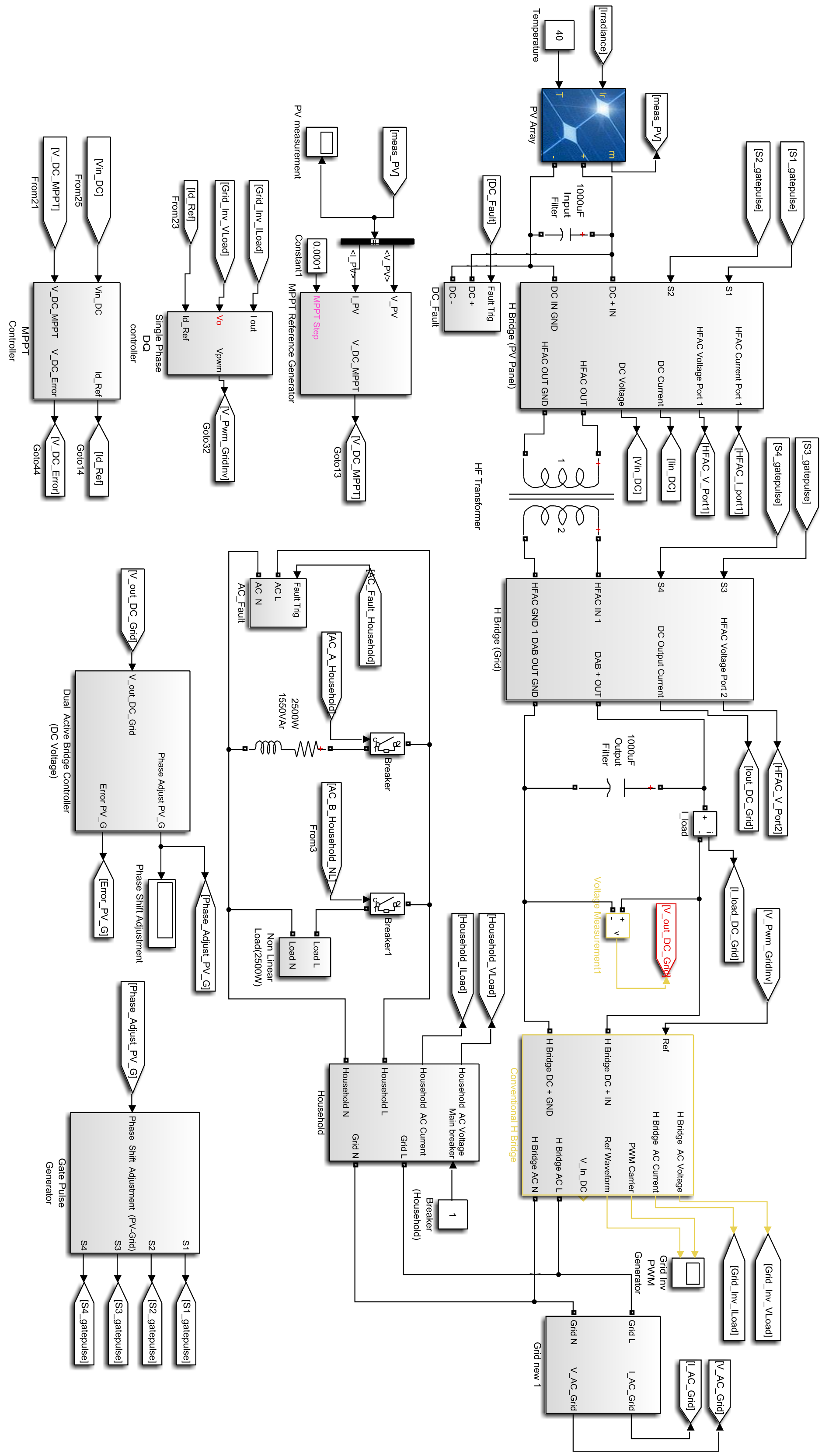

Appendix D: Simulink model-DAB inverter (load at PV array side)

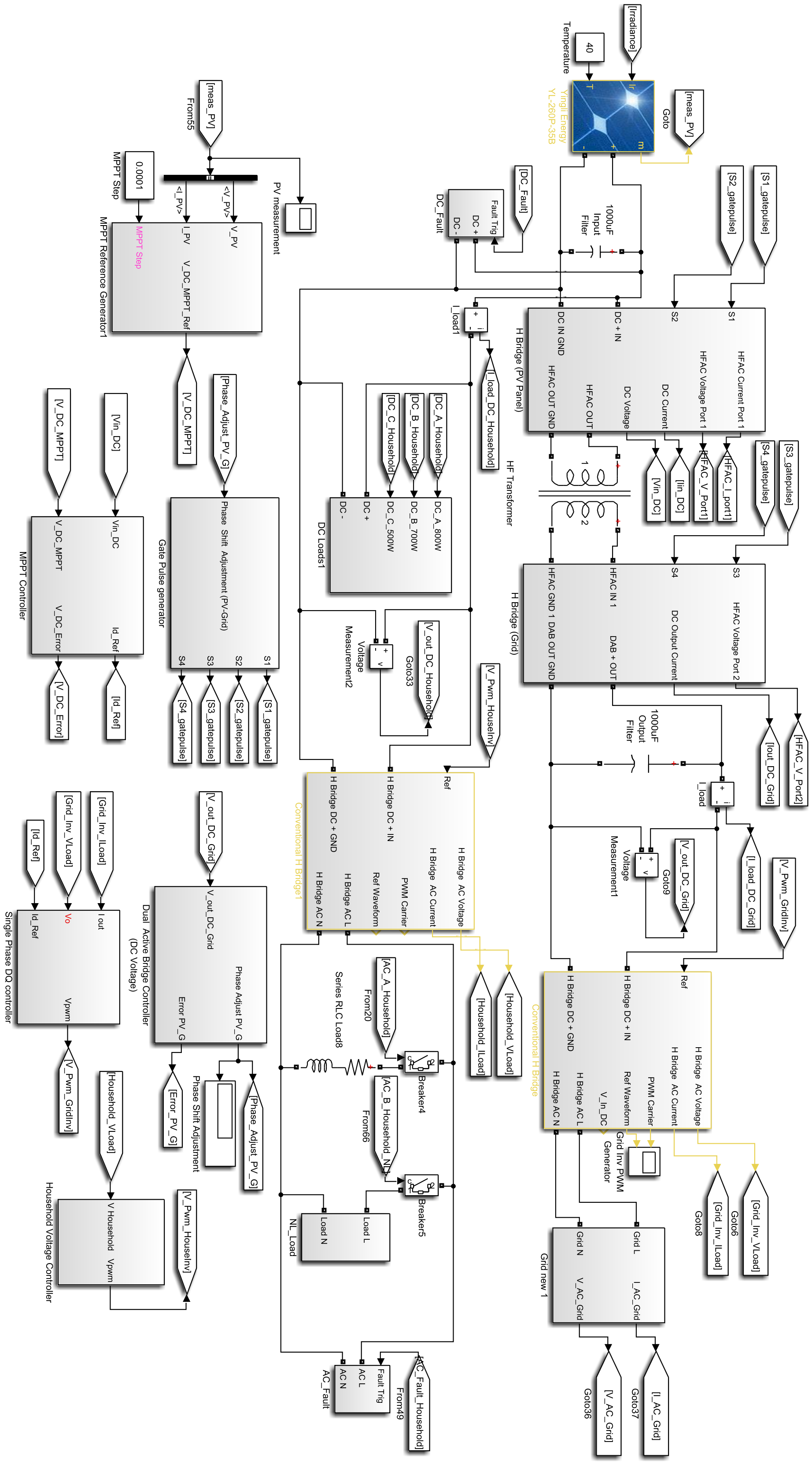

Appendix E: MATLAB code for the mathematical model of the TAB

```
clear all
clc
syms n t
syms V_h % comment out when plotting household side voltage

%no of Fourier terms

N=30;

%winding resistances

R_pv=10e-3;
R_h=10e-3;
R_g=10e-3;

%leakage inductances

f=20000;
L_pv=25e-6;
L_h=25e-6;
L_g=25e-6;

%phase shifts

delta_pv=30;
delta_g=60;
delta_h=70;

RL_g=10;
RL_h=10;
C_g=1e-3;
C_h=1e-3;

V_pv=420;
% V_h=350; %uncomment when plotting currents
V_g=350;

%Hz to rad/s

Ws=2*pi*f;
%W=(2*n+1)*Ws;

%delta pi transformation

Zpvh=((R_pv+j*Ws*L_pv)*(R_h+j*Ws*L_h)+(R_pv+j*Ws*L_pv)*(R_g+j*Ws*L_g
)+(R_h+j*Ws*L_h)*(R_g+j*Ws*L_g))/(R_g+j*Ws*L_g);
Zpvg=((R_pv+j*Ws*L_pv)*(R_h+j*Ws*L_h)+(R_pv+j*Ws*L_pv)*(R_g+j*Ws*L_g
)+(R_h+j*Ws*L_h)*(R_g+j*Ws*L_g))/(R_h+j*Ws*L_h);
Zgh=((R_pv+j*Ws*L_pv)*(R_h+j*Ws*L_h)+(R_pv+j*Ws*L_pv)*(R_g+j*Ws*L_g)
+(R_h+j*Ws*L_h)*(R_g+j*Ws*L_g))/(R_pv+j*Ws*L_pv);

Rpvh=real(Zpvh);
```

```
Rpvg=real(Zpvg);
Rgh=real(Zgh);

Lpvh=imag(Zpvh)/Ws;
Lpvg=imag(Zpvg)/Ws;
Lgh=imag(Zgh)/Ws;

%deg to rad transformation

d_pv=delta_pv*pi/180;
d_h=delta_h*pi/180;
d_g=delta_g*pi/180;

%mathermatical model

Zn_pvh=(sqrt(Rpvh^2+((2*n+1)*Ws*Lpvh)^2));
Psin_pvh=(atan(((2*n+1)*Ws*Lpvh)/Rpvh));
Zn_gh=(sqrt(Rgh^2+((2*n+1)*Ws*Lgh)^2));
Psin_gh=(atan(((2*n+1)*Ws*Lgh)/Rgh));
Zn_pvg=(sqrt(Rpvg^2+((2*n+1)*Ws*Lpvg)^2));
Psin_pvg=(atan(((2*n+1)*Ws*Lpvg)/Rpvg));



IL_pvh_tot=((1/(2*n+1))*((((V_pv)/Zn_pvh)*sin((2*n+1)*(Ws*t-d_pv)-
Psin_pvh))-(((V_h)/(Zn_pvh))*sin((2*n+1)*(Ws*t-d_h)-Psin_pvh))));
IL_pvh=(4/pi)*symsum(IL_pvh_tot, n, 0, N);

IL_pvg_tot=((1/(2*n+1))*((((V_pv)/Zn_pvg)*sin((2*n+1)*(Ws*t-d_pv)-
Psin_pvg))-(((V_g)/(Zn_pvg))*sin((2*n+1)*(Ws*t-d_g)-Psin_pvg))));
IL_pvg=(4/pi)*symsum(IL_pvg_tot, n, 0, N);

IL_gh_tot=-((1/(2*n+1))*((((V_h)/Zn_gh)*sin((2*n+1)*(Ws*t-d_h)-
Psin_gh))-(((V_g)/(Zn_gh))*sin((2*n+1)*(Ws*t-d_g)-Psin_gh))));
IL_gh=(4/pi)*symsum(IL_gh_tot, n, 0, N);

%transformer output and input currents

IL_pv=(IL_pvg+IL_pvh);
IL_h=(IL_pvh+IL_gh);
IL_g=(IL_pvg-IL_gh);

IL_pv_sW_tot=(1/(2*n+1))*sin((2*n+1)*(Ws*t-d_pv));
IL_pv_sW=(4/pi)*symsum(IL_pv_sW_tot, n, 0, N);

IL_h_sW_tot=(1/(2*n+1))*sin((2*n+1)*(Ws*t-d_h));
IL_h_sW=(4/pi)*symsum(IL_h_sW_tot, n, 0, N);

IL_g_sW_tot=(1/(2*n+1))*sin((2*n+1)*(Ws*t-d_g));
IL_g_sW=(4/pi)*symsum(IL_g_sW_tot, n, 0, N);

%converter output and input currents

IL_pv_out=IL_pv_sW*IL_pv;
```

```
IL_h_out=IL_h_sW*IL_h;
IL_g_out=IL_g_sW*IL_g;

I_h_simp_tot=(1/(2*n+1)^2)*((V_pv*cos((2*n+1)*(d_pv-
d_h)+Psin_pvh)/(Zn_pvh))-
(V_h*(((cos(Psin_pvh))/(Zn_pvh))+((cos(Psin_gh))/(Zn_gh))))+(V_g*cos
((2*n+1)*(d_g-d_h)+Psin_gh)/(Zn_gh)));
I_h_simp=(8/(pi^2))*symsum(I_h_simp_tot, n, 0, N);

I_g_simp_tot=(1/(2*n+1)^2)*((V_pv*cos((2*n+1)*(d_pv-
d_g)+Psin_pvg)/(Zn_pvg))-
(V_g*(((cos(Psin_pvg))/(Zn_pvg))+((cos(Psin_gh))/(Zn_gh))))+(V_h*cos
((2*n+1)*(d_h-d_g)+Psin_gh)/(Zn_gh)));
I_g_simp=(8/(pi^2))*symsum(I_g_simp_tot, n, 0, N);

% fplot(IL_pv,[0,0.0002])  %uncomment to plot currents
% hold all
%

%household side and grid side voltages

V_h_c = -((V_h)/(RL_h*C_h))+(1/C_h)*IL_h_out;           %comment out
when plotting currents
V_h_csimplfd = -((V_h)/(RL_h*C_h))+(1/C_h)*I_h_simp;      %comment
out when plotting currents
%
% V_g_c = -((V_g)/(RL_g*C_g))+(1/C_g)*IL_g_out;
% V_g_csimplfd = -((V_g)/(RL_g*C_g))+(1/C_g)*I_g_simp;
%
%
opts = odeset('MaxStep',50e-8);
F = matlabFunction(V_h_c,'vars',{'t','V_h'});
[t,V_h] = ode113(F,[0 0.2],0,opts);


plot(t,V_h)
hold all
```

Appendix F: Simulink model -TAB inverter